THE ASTROPHYSICAL JOURNAL, 277:623–633, 1984 February 15

THE NEAR-INFRARED CONTINUUM EMISSION OF VISUAL REFLECTION NEBULAE

K. SELLGREN[1,2]
California Institute of Technology
Received 1983 May 9; accepted 1983 August 8

ABSTRACT

The near-infrared emission of the visual reflection nebulae NGC 7023, 2023, and 2068 is found to consist of a smooth continuum from 1.25 to 4.8 μm, characterized by a color temperature of $\sim$1000 K, and strong emission features at 3.3 and 3.4 μm. The spectrum is the same in all three sources, and is independent of position over regions 0.4–0.9 pc in diameter within each source. The 2.2 μm surface brightness distributions in NGC 7023 and 2023 agree well with the distributions of visual reflected light. The near-infrared emission, however, cannot be explained by reflected light, fluorescence, faint stars, free-free emission, or by thermal emission from dust in equilibrium with the stellar radiation field.

A model is proposed in which the emission is due to thermal emission from very small grains (radius $\sim$10 Å) which are briefly heated to $\sim$1000 K by absorption of individual ultraviolet photons. This model explains the agreement between near-infrared and visual surface brightness distributions, and the constancy of the energy distribution with offset from the central stars. The number of grains with $\sim$10 Å radius required by the observations is in agreement with the numbers expected from an extrapolation of the grain size distribution of Mathis, Rumpl, and Nordsieck to smaller grain sizes.

Subject headings: infrared: sources — interstellar: grains — nebulae: reflection

I. INTRODUCTION

Reflection nebulae have provided in the past an astrophysical laboratory well suited for the study of the reflection properties of interstellar dust grains at visual and ultraviolet wavelengths. The observations of this paper were begun with the goal of extending to near-infrared wavelengths the study of grains in reflection. Three classical visual reflection nebulae, NGC 7023, 2023, and 2068, were observed between 1.25 and 2.2 μm. Soon two mysteries were uncovered: all three nebulae had similar near-infrared colors, despite widely different colors of their illuminating stars, and two of the nebulae were much brighter at 2.2 μm than could be easily explained by reflected light. Observations were subsequently obtained of the nebulae at longer wavelengths (Sellgren, Werner, and Dinerstein 1983*a*, hereafter Paper I) and of the 2.2 μm polarization (Sellgren, Werner, and Dinerstein 1983*b*). These observations showed that the near infrared extended emission of these nebulae (1) consisted of a smooth continuum whose spectrum could be characterized by a color temperature of $\sim$1000 K; (2) showed the unidentified 3.3 and 3.4 μm features, seen in many other infrared sources, in emission; (3) had a 2.2 μm polarization much lower than was expected for reflected light; and (4) had a surface brightness at 3.8 μm far in excess of what could be explained by reflected light, for all three nebulae. A number of emission mechanisms were considered briefly in Paper I, most of which were found to be unlikely. The most viable mechanisms discussed were thermal emission from dust grains with ratios of infrared to ultraviolet emissivities much lower than is usually found from observations or theory; thermal emission from grains small enough to be heated briefly to high temperatures, by individual ultraviolet (UV) photons or by collisions; and fluorescent mechanisms producing a continuum.

This paper presents near-infrared mapping, photometry, and spectrophotometry of these three nebulae, in order to expand on the observations of Paper I and to provide as much observational insight into the phenomenon of the unexplained continuum emission as possible. A wide variety of possible emission mechanisms are also discussed, with the aim of understanding the source of the emission, and its implications for the composition of the interstellar medium. To date no satisfactory explanation of all the observations is available.

II. OBSERVATIONS

Observations of NGC 7023 in 1979 August and 1981 July, and of NGC 2023 and NGC 2068 in 1981 January–February and 1981 October, were made using the 24 inch (61 cm) telescope at Mount Wilson Observatory. Diaphragms of 30″ and 60″ diameter were used. The spacing between source and sky positions was 3′ in right ascension in 1979 and 6′ in right ascension in 1981. An InSb detection system was used to obtain nebular surface photometry at wavelengths of 1.25 μm (J), 1.65 μm (H), and 2.2 μm (K). The positional uncertainties of the surface brightness maps are estimated to be $\pm$4″.

The Mount Wilson Observatory 60 inch (1.5 m) telescope was used to obtain spectrophotometry, from 1.5 to 2.5 μm with $\Delta\lambda/\lambda = 0.05$, of HD 200775, the central star of NGC 7023, in 1979 November and 1980 June, and of the NGC 7023 nebula, 23″ north and 14″ west of HD 200775, in 1980 June. A circular variable filter wheel cooled to 77 K was used.

[1] Observations made partially at the Mount Wilson Observatory, Carnegie Institution of Washington, as part of a collaborative agreement between Carnegie Institution of Washington and California Institute of Technology.

[2] Visiting Astronomer at the Infrared Telescope Facility, which is operated by the University of Hawaii under contract from the National Aeronautics and Space Administration.

The nebular measurements were made with a 16″ diameter diaphragm and 77″ spacing in right ascension between source and sky positions. Broad-band photometry at 1.25, 1.65, and 2.2 μm was also obtained for star and nebula.

The Infrared Telescope Facility at Mauna Kea Observatory was used to obtain spectrophotometry, between 1.9 and 3.7 μm with $\Delta\lambda/\lambda = 0.01$, of the central stars of NGC 7023, 2023, and 2068 in 1982 October, as well as broad-band photometry at 1.25 μm, 1.65 μm, 2.2 μm, 3.5 μm (L), 3.8 μm (L'), and 4.8 μm (M). A 12″ diameter diaphragm and a spacing in right ascension of 2′–3′ between source and sky positions was used. A circular variable filter wheel at 77 K was used for the spectrophotometry. Spectrophotometry between 1.9 and 3.7 μm and photometry at 1.25, 1.65, 2.2, 3.8, and 4.8 μm was also obtained at various positions in the three nebulae.

The surface brightness photometry and spectrophotometry of NGC 7023 required correction for instrumental scattered light from HD 200775. This correction, of order 10%–20%, was determined by observations of isolated bright stars, and has been applied to all observations of NGC 7023 reported in this paper.

The observed nebular surface brightnesses were corrected for the contributions of field stars found in 2.2 μm scans of NGC 7023, 2023, and 2068 by Sellgren (1983*a*, hereafter Paper II), using the stellar magnitudes and positions listed there. In NGC 2068 the observations of Strom, Strom, and Vrba (1976) were also included in correcting for field stars.

All observations were calibrated using the standard stars of Elias *et al.* (1982) and Neugebauer (1982). Since L' and M magnitudes were not available in all cases, the L magnitude was adopted at longer wavelengths for a few stars of spectral type A or earlier. The flux densities for zero magnitude listed by Beckwith *et al.* (1976) and Neugebauer *et al.* (1979) were adopted. The photometric filters used are described in Paper I and by Neugebauer *et al.* (1982), expect for the L filter, which has $\lambda = 3.50$ μm and $\Delta\lambda = 1.05$ μm. The spectrophotometry with 1% and 5% resolution was calibrated assuming that the early-type standard stars could be approximated by 9700 K blackbodies normalized to the 2.2 μm broad-band point. No correction for Brackett-γ absorption in the standard stars was made. This correction should be 3% or less for the stars used to calibrate the 1% resolution spectrophotometry, 1% or less for the 5% resolution spectrophotometry, and negligible in all cases for the 2.2 μm broad-band filter (Elias 1978).

III. RESULTS

In Paper I photometry at 2.2, 3.8, and 4.8 μm, and spectrophotometry from 1.9 to 3.7 μm, were presented for a few positions in NGC 7023, 2023, and 2068. This paper expands the observations of these sources to include surface brightness maps at 2.2 μm, photometry at many positions at 1.25 and 1.65 μm, and spectrophotometry extending the shortest wavelength observed with medium resolution to 1.5 μm. These additional observations strengthen the conclusions of Paper I, showing the near-infrared emission extends over regions 3′–6′ in diameter with the same 1.25–4.8 μm energy distribution at all positions. This section discusses the results of the observations of reflection nebulae in detail, including comparisons with observations at visual, mid-infrared, and far-infrared wavelengths.

a) The Spatial Distribution

The maps of the surface brightness of NGC 7023 at 2.2 and 1.65 μm are shown in Figure 1, while the maps of the surface brightnesses of NGC 2023 and NGC 2068 at 2.2 μm are shown in Figure 2. The 2.2 and 1.65 μm surface brightness distributions of NGC 7023 resemble each other closely. The integrated

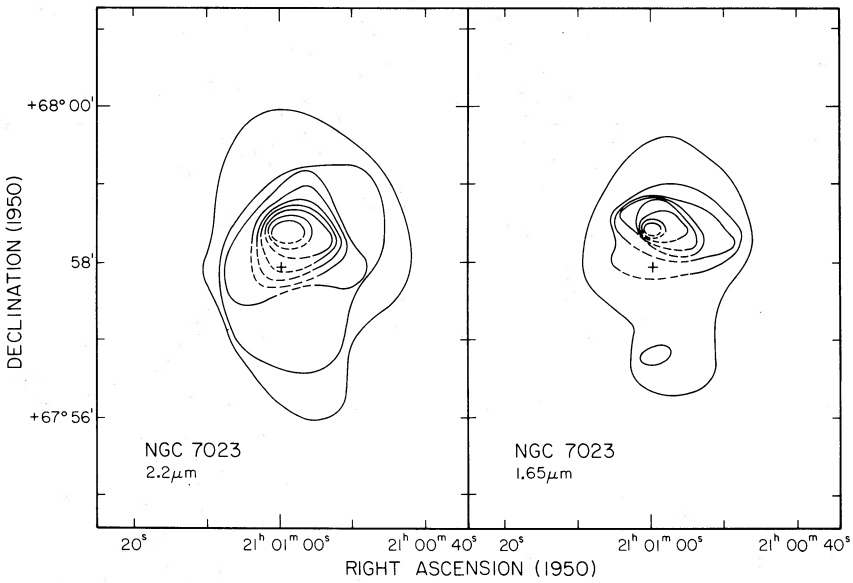

FIG. 1.—Surface brightness maps of NGC 7023 at 2.2 μm and 1.65 μm. Diaphragms of 30″ and 60″ diameter were used. The position of HD 200775 is marked with a cross. Observations could not be made closer than 30″ from HD 200775; contours within this radius have been completed with dashed lines. The surface brightness has been corrected for the contributions of stars found at 2.2 μm in the nebula (Paper II), and for instrumental scattering of light from HD 200775. The contour intervals are 50 mJy into a 60″ diameter diaphragm at both 2.2 and 1.65 μm. The 1 σ uncertainties in the surface brightness are 9–13 mJy per 60″ diaphragm at 2.2 μm, and 4–17 mJy per 60″ diaphragm at 1.65 μm.

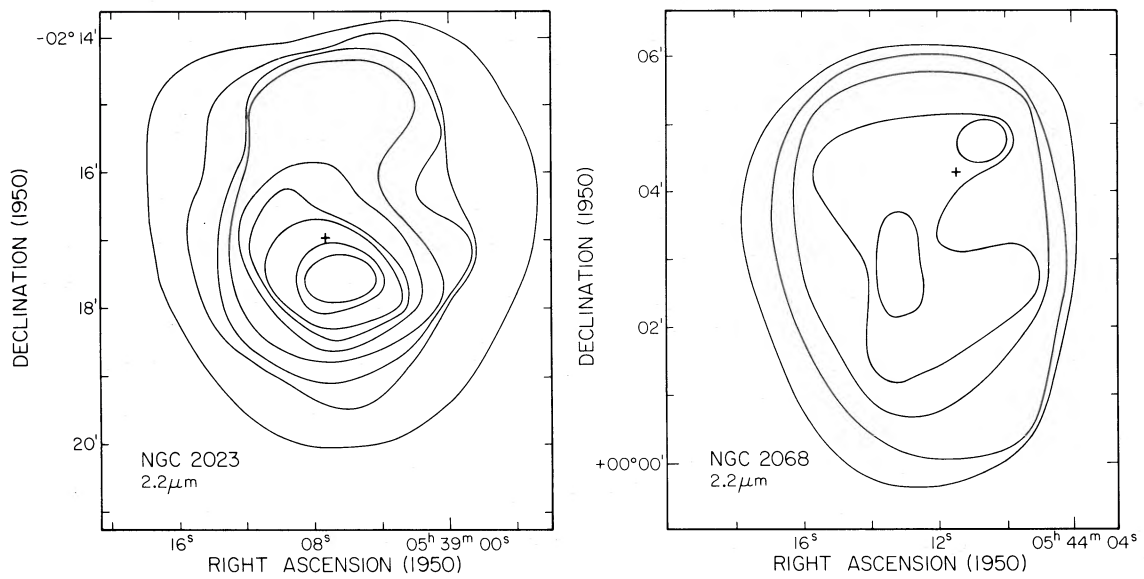

FIG. 2.—Surface brightness maps of NGC 2023 and NGC 2068 at 2.2 μm. A 60″ diameter diaphragm was used. The positions of HD 37903 and HD 38563N are marked with a cross in NGC 2023 and NGC 2068, respectively. The surface brightness has been corrected for the contributions of stars found at 2.2 μm in these nebulae (Paper II). The contours in NGC 2023 are 25, 50, 75, 100, 150, 200, 250, 300, and 350 mJy into a 60″ diaphragm. The contour interval in NGC 2068 is 25 mJy into a 60″ diaphragm. The 1 σ uncertainty in the 2.2 μm surface brightness of NGC 2023 and NGC 2068 is 7 mJy per 60″ diaphragm.

2.2 μm flux densities of the nebulae, excluding the contributions of their illuminating stars and other field stars, are 1.5, 4.1, and 3.0 Jy for NGC 7023, 2023, and 2068, respectively.

In NGC 7023, 2023, and 2068, respectively, five, two, and six of the stars whose contributions were subtracted from the near infrared surface photometry are pre–main-sequence stars (Paper II) which may be or are variable. Positions containing contributions from known pre-main-sequence stars were given lower weight or ignored in the analysis. Additional uncertainties in the photometry arise from the high surface density of stars near the centers of the stellar clusters. The near-infrared surface brightness of NGC 2068 (Fig. 2) is uncertain by typically ±1 contour interval within a radius of ~1′ from its central star, due to the combined positional uncertainties of the stellar and nebular positions. The uncertainties due to star subtraction in any of the nebulae should not affect the general surface brightness level, extent, and integrated flux densities of the near-infrared maps, or the average properties of the near-infrared colors.

The near-infrared, far-infrared, and visual surface brightness distributions are similar in NGC 7023 and NGC 2023, sharing in common the general locations of the peak surface brightnesses, north and south of the central star for NGC 7023 and 2023, respectively, the general extent of the emission, and the bar of emission 1′ south of the star in NGC 7023. The visual radiation from the nebulae is starlight from the central stars reflected by dust grains in the surrounding molecular clouds, while the far-infrared emission (Whitcomb *et al.* 1981; Harvey, Thronson, and Gatley 1980) is due to thermal radiation from dust grains at temperatures of 40–60 K.

A quantitative comparison of the distribution of visual and near infrared emission in NGC 7023 and 2023 can be found in Figures 3 and 4, which show at 0.55 μm and 2.2 μm the nebular surface brightness as a function of angular offset from the visual illuminating stars. The ratio of surface brightnesses at 0.55 μm and 2.2 μm in these two nebulae is remarkably constant, generally varying by no more than a factor of 2, over regions where the absolute values of the visual and infrared surface brightnesses vary by a factor of ~20.

The ratio of visual (V) and 2.2 μm (K) surface brightnesses additionally has a similar value in NGC 7023 and NGC 2023. For NGC 7023 $V-K=2.7$ mag, while $V-K=3.2$ mag for NGC 2023, where these are average values in the nebulae. In NGC 2068, at one position observed at visual wavelengths by Zellner (1970), $V-K=2.8$ mag, in good agreement with the average values for NGC 7023 and NGC 2023.

b) *The Energy Distribution*

Near-infrared spectra at selected positions in NGC 7023 and 2023 are shown in Figure 5. These spectra clearly show that the near-infrared emission of these nebulae is characterized by a smooth continuum from 1.5 to 3.7 μm, a strong emission feature at 3.3 μm, and a broad emission wing near 3.4 μm. The emission features at 3.3 and 3.4 μm are two of six unidentified infrared emission features, whose observed properties have been reviewed by Aitken (1981) and Willner (1983). The broad-band photometry at 1.25 and 4.8 μm agrees well with extrapolations of the continuum observed between 1.5 and 3.7 μm, suggesting that the smooth continuum extends at least from 1.25 to 4.8 μm.

The near-infrared spectra of NGC 7023 and NGC 2023 shown in Figure 5 resemble each other strongly, and this similarity extends to other nebular positions observed. The color temperature defined by the broad-band observations at 2.2 and 3.8 μm in NGC 7023, 2023, and 2068 appears to be the same, ~1000 K, for all nebulae, and is independent of position within each nebula (Paper I). The 3.3 μm feature-

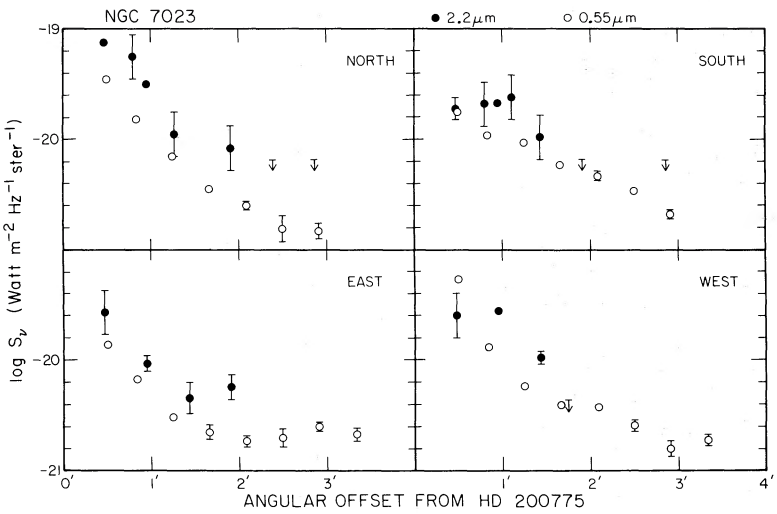

FIG. 3.—The surface brightness S_ν of NGC 7023 at 2.2 μm (*filled circles*) and 0.55 μm (*open circles*) vs. angular offset from HD 200775, north, south, east, and west of this star. The 2.2 μm data are from this paper, using 30″ and 60″ diameter diaphragms; the 0.55 μm data are from Witt and Cottrell (1980), who used a 50″ diameter diaphragm. Error bars represent ± 1 σ uncertainties, and are shown only when larger than ± 0.03 in the log. Upper limits are 3 σ upper limits at 2.2 μm. The surface brightnesses are given as W m^{-2} Hz^{-1} sr^{-1} at 2.2 μm and 0.55 μm. Positions with error bars in log S_ν of ± 0.2 are positions where 2.2 μm data were not directly available. At these positions the 2.2 μm surface brightness was estimated from the 2.2 μm contour map, estimated from a 1.65 μm measurement using an average ratio of 2.2 μm to 1.65 μm surface brightnesses, or was measured directly at 2.2 μm but was corrected for the contribution of a pre-main sequence star which may be variable.

to-continuum ratio also appears to be constant at a value of ~ 6 in each of these nebulae, at all positions observed (Paper I).

The colors at shorter wavelengths are also apparently independent of position. The results of surface photometry at 1.25 μm (J), 1.65 μm (H), and 2.2 μm (K) in the three reflection nebulae are shown in Figure 6. The colors (Paper II) of stars in the nebulae, including the stars which illuminate the visual reflection nebulosity, are also shown in Figure 6 for comparison. The near-infrared colors of the reflection nebulae are extremely different from the colors of the stars within the reflection nebulae.

The observed $J-H$ and $H-K$ colors of NGC 7023, 2023, and 2068 are plotted versus projected radial offset from the visual illuminating stars in Figure 7. The values of $J-H$ and $H-K$ are clearly independent of projected radial distance in NGC 7023 and NGC 2068. There may be a suggestion of a color gradient in NGC 2023, but the present evidence is not convincing, and further observations would be needed to verify it. The generally good agreement of the

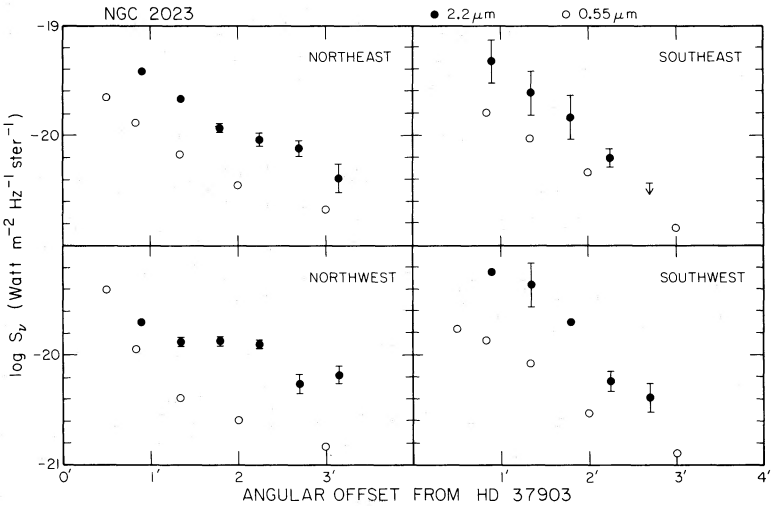

FIG. 4.—The surface brightness S_ν of NGC 2023 at 2.2 μm (*filled circles*) and 0.55 μm (*open circles*) vs. angular offset from HD 37903, along lines at 45° to the cardinal directions, northeast, southeast, northwest, and southwest of this star. The 2.2 μm data are from this paper, using a 60″ diameter diaphragm; the 0.55 μm data are from Witt, Schild, and Kraiman (1983), who used a 50″ diameter diaphragm. Error bars represent ± 1 σ uncertainties, and are shown only when larger than ± 0.03 in the log. The upper limit is a 3 σ upper limit at 2.2 μm. The surface brightnesses are given as W m^{-2} Hz^{-1} s^{-1} at 2.2 μm and 0.55 μm. Positions with error bars in log S_ν of ± 0.2 are positions where the 2.2 μm data were corrected for the contribution of a pre-main sequence star which may be variable.

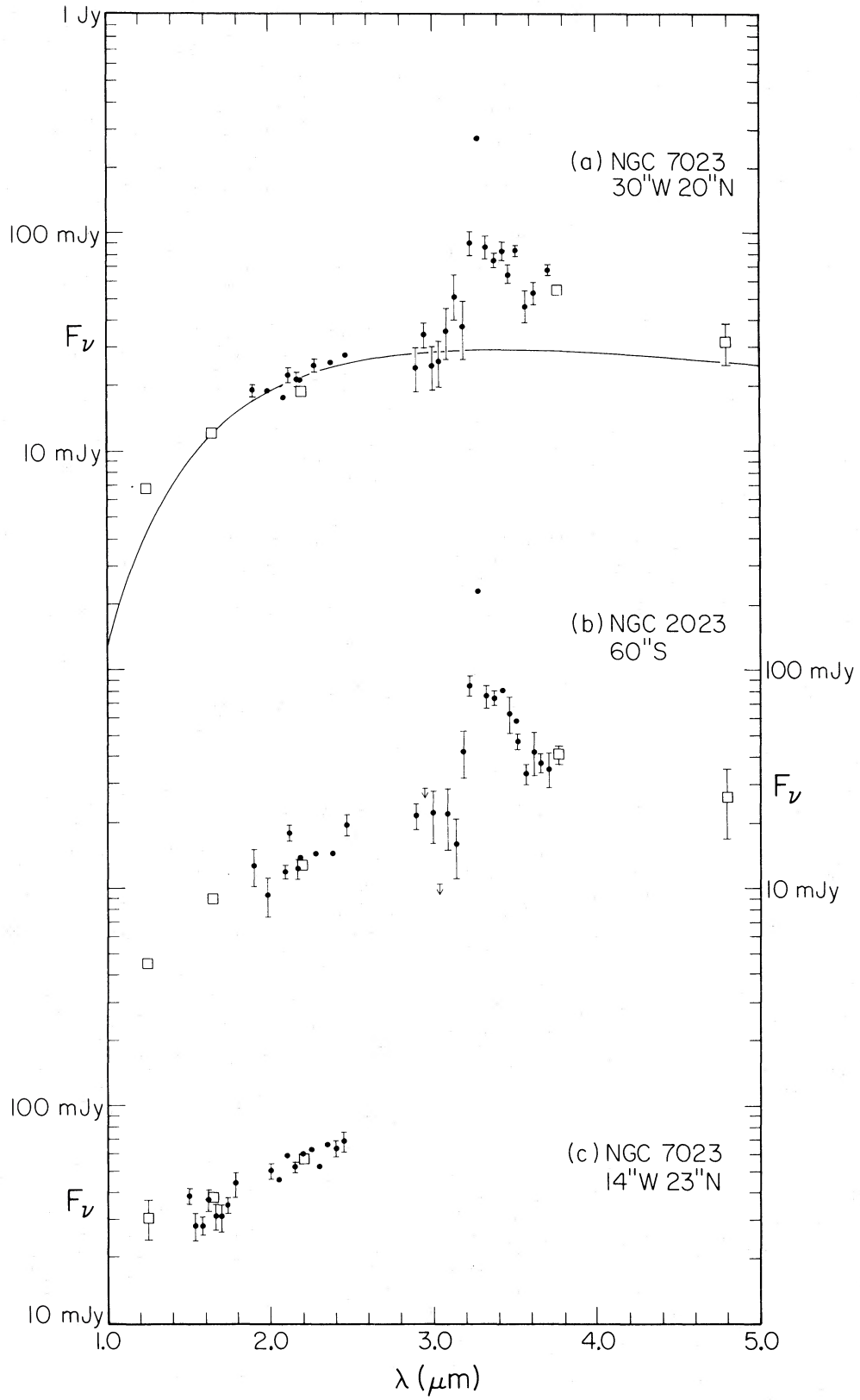

FIG. 5.—The near-infrared spectra of positions in NGC 7023 and NGC 2023. The positions observed are (*a*) 30″ west 20″ north of HD 200775 in NGC 7023; (*b*) 60″ south of HD 37903 in NGC 2023; and (*c*) 14″ west 23″ north of HD 200775 in NGC 7023. The filled circles are spectrophotometry with 1% (*a*, *b*) or 5% (*c*) resolution. The open squares are broad-band photometric measurements. The solid curve shown in one spectrum (*a*) is a 1500 K gray body normalized to the 1.65 μm broad-band point. Error bars represent ±1 σ uncertainties and are only shown when larger than ±5%. Upper limits are 3 σ upper limits on the spectrophotometry. The 4.8 μm broadband photometry of NGC 2023 (*b*) is a 2.8 σ measurement. The units are flux density within the diaphragm size used, which was 12″ (*a*, *b*) or 16″ (*c*) in diameter. The observations are from this paper and Paper I.

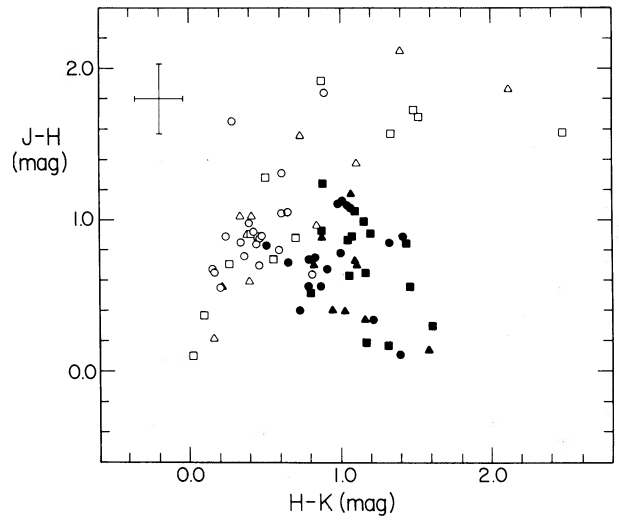

FIG. 6.—The $J-H$ colors plotted vs. the $H-K$ colors for nebular positions and stars in NGC 7023 (*circles*), NGC 2023 (*squares*), and NGC 2068 (*triangles*). Nebular colors are shown as filled symbols, while stellar colors (Paper II) are shown as open symbols. Error bars representing typical $\pm 1\ \sigma$ uncertainties for the nebular observations are shown in the upper left-hand corner; the uncertainties in the stellar colors are much smaller.

observed colors of NGC 7023, 2023, and 2068 seen in Figure 7 emphasize the similarity of nebular colors at all positions.

The conclusion that the nebular energy distribution is independent of position within the nebula makes it possible to use integrated flux densities at 2.2 μm for each nebula, combined with an average nebular energy distribution, to determine the total flux density of the nebulae at wavelengths between 1.25 and 4.8 μm. The total energy distribution of each nebula is shown in Figure 8, in units of the flux per logarithmic frequency interval. This figure demonstrates that the near-infrared emission from 1.25 to 4.8 μm is a small fraction of the total luminosity of the nebulae. Most of the nebular energy is emitted at far-infrared wavelengths as thermal radiation from dust at temperatures of 40–60 K. The far-infrared luminosity is typically 30%–50% of the stellar luminosity, while the near-infrared emission accounts for only $\sim 1\%$ of the stellar luminosity.

c) *The Central Stars*

The photometry and spectrophotometry of the central stars of the reflection nebulae are shown in Figure 9. The spectra of these stars are featureless, as expected, except for weak 3.3 μm emission in the central star of NGC 2023, with a feature-to-continuum ratio of 0.35, presumably due to the contribution of the nebular emission within the 12″ diaphragm. Upper limits of 0.15 can be placed on the 3.3 μm feature-to-continuum ratios in HD 200775 and HD 38563N. The 2.2 μm surface brightnesses near the central stars inferred from the 3.3 μm feature-to-continuum ratios are consistent with a smooth interpolation of the 2.2 μm surface brightness maps. The detection of a nebular contribution to near-infrared measurements of HD 37903 with a 12″ diaphragm implies care must be taken, as has been noted by Guetter (1979), with both the diaphragm size and separation of source and sky positions when determining the extinction curves of early-type stars near molecular clouds, especially when the value of $R = A_V/E(B-V)$ is inferred from the longest wavelength photometry obtained.

IV. DISCUSSION

a) *Overview of the Problem*

The main features of the near-infrared observations of these visual reflection nebulae that must be explained are the spatial distribution and the energy distribution of the emission. The near-infrared surface brightness distributions in two of the nebulae show strong peaks near the illuminating star of the visual reflection nebula and agree with the surface brightness distributions of the visual reflected light. The energy distribution consists of a smooth continuum from 1.25 to 4.8 μm which is characterized by a color temperature of ~ 1000 K, in addition to the unidentified 3.3 and 3.4 μm emission features; the spectrum is seen to be the same in all three nebulae and to be independent of position or distance from the central star within each nebula, over a region 3′–6′ in diameter, or 0.4–0.9 pc, at the distances (Viotti 1969; Lee 1968) of these nebulae.

The observations above, and in particular the source of the near-infrared continuum emission, are not easily understood. Five mechanisms have been studied in detail by Sellgren (1983*b*) and were found to be unable to explain the continuum emission. Section IV*b* presents a possible model which may explain the observations. I would like to emphasize that the true explanation may prove to be none of the mechanisms discussed in this paper.

The mechanisms for producing the near-infrared continuum emission discussed by Sellgren (1983*b*) are equilibrium thermal emission, fluorescence, reflected light, stars, and free-free emission. A brief summary of the reasons why these mechanisms can be ruled out is given here; further details are given in Sellgren (1983*b*).

Equilibrium thermal emission is ruled out by the high value of the observed color temperature, ~ 1000 K, at distances $\gtrsim 0.1$ pc from a moderate luminosity B star. Thermal emission from dust with very low ratios of infrared to ultraviolet emissivities, $Q_{IR}/Q_{UV} \sim 10^{-7}$, would account for the observed color temperature, but would then be inconsistent with the observed spatial distribution of the emission and fail to explain the constancy of the observed color temperature with distance from the central star. Fluorescent processes may produce line emission, such as has been proposed for the 3.3 and 3.4 μm emission features (Allamandola, Greenberg, and Norman 1979), but are unable to produce the remaining smooth, featureless continuum over the factor of 4 in wavelength observed, from 1.25 to 4.8 μm, and also require an unreasonably high conversion efficiency of UV to infrared photons. Reflected light can be ruled out because the observed integrated nebular flux densities, at 2.2 μm in NGC 2023 and 2068, are larger than the dereddened 2.2 μm flux densities of the stars which illuminate the visual reflection nebulae; and because the 3.8 μm surface brightness observed in positions in all three nebulae is too large by factors of 2–30 to be explained by reflected light. The difference between the observed nebular colors and stellar colors of Paper II, as well as predictions (Sellgren 1983*b*) of the surface brightness due

to faint stars, rule out undetected stars as significant contributors to the observed nebular emission. Free-free emission can be ruled out because of the low values of observed radio continuum emission in the nebulae.

b) A Thermal Fluctuation Model

A number of authors (Duley 1973; Greenberg and Hong 1974; Harwit 1975; Allen and Robinson 1975; Purcell 1976) have suggested that the temperature of small grains may fluctuate strongly under interstellar heating conditions, due to their small heat capacity. This mechanism may offer a plausible explanation for the observed near infrared emission.

The heat capacity C_V of a grain is most often approximated by the Debye theory. In the applications previously considered, a typical grain in a dark cloud, whose equilibrium temperature of 10–15 K is determined by the interstellar radiation field, is briefly heated to much higher temperatures after absorption of a UV photon (Duley 1973; Greenberg and Hong 1974; Harwit 1975; Purcell 1976) or upon formation of a chemical bond between molecules on the grain surface (Allen and Robinson 1975). These authors found peak grain temperatures lower than the Debye temperatures of typical grain materials, 200–500 K (Allen and Robinson 1975), so that the low-temperature approximation to the heat capacity, $C_V \propto T^3$, was appropriate. At the higher temperatures characteristic

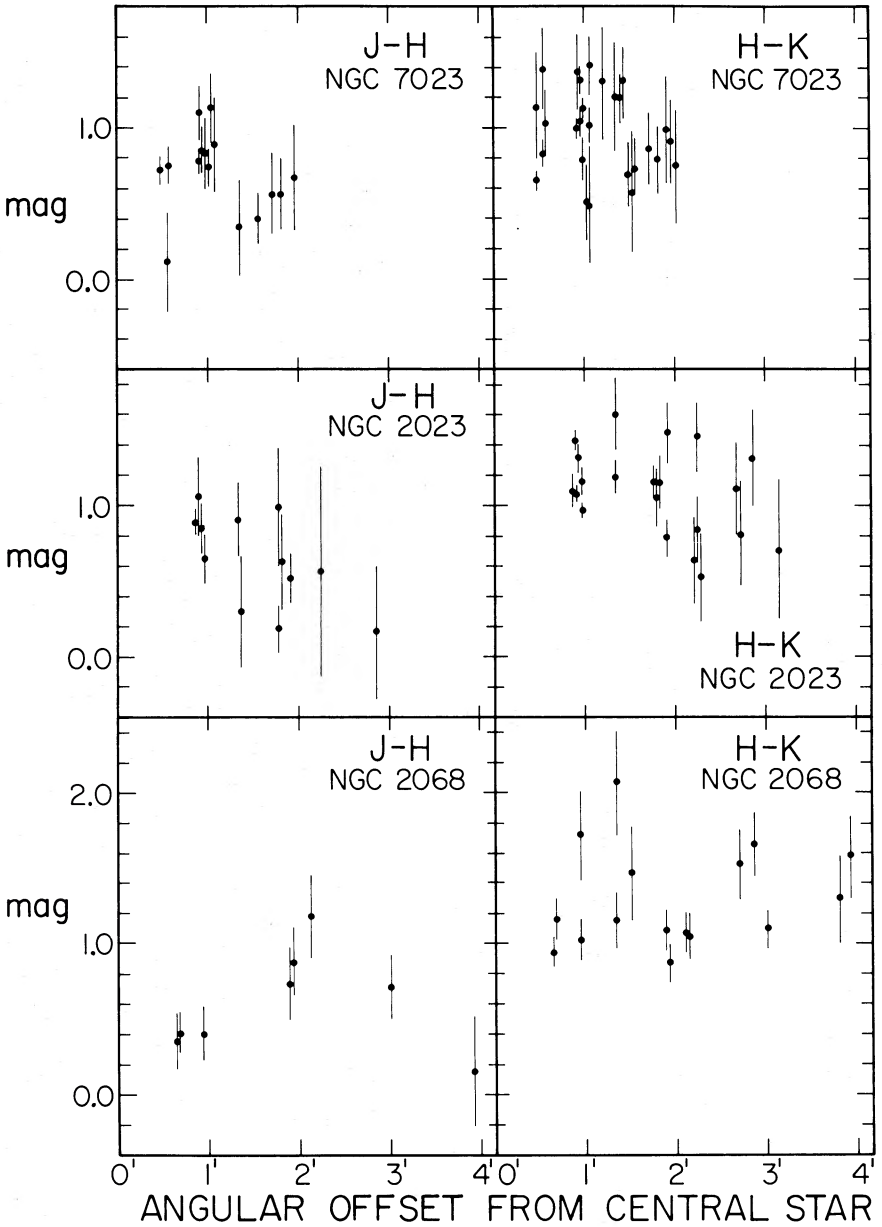

FIG. 7.—The $J-H$ and $H-K$ colors of nebular positions in NGC 7023, NGC 2023, and NGC 2068 plotted vs. angular offset from the illuminating star of each reflection nebula. The error bars represent $\pm 1\ \sigma$ uncertainties.

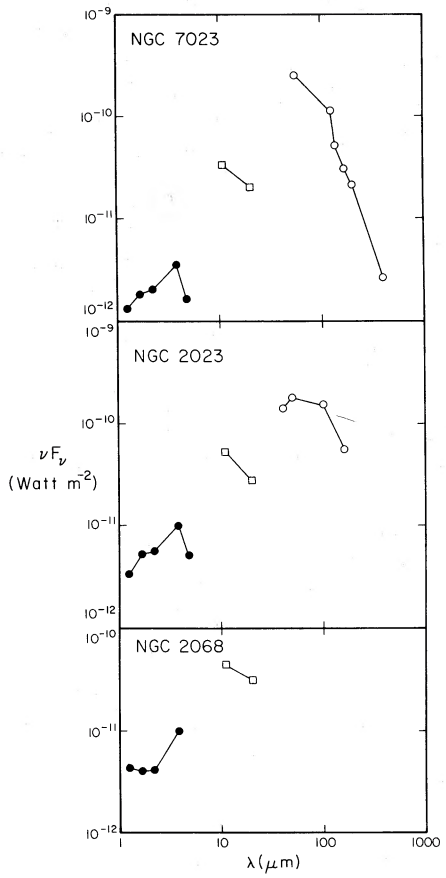

FIG. 8.—The energy distributions of NGC 7023 (*top*), NGC 2023 (*middle*), and NGC 2068 (*bottom*). Filled circles are near-infrared measurements derived from the integrated 2.2 μm flux density of each nebula (this paper) and the ratios of surface brightnesses at 1.25, 1.65, 3.8, and 4.8 μm to that at 2.2 μm, at each nebular peak (this paper and Paper I). The open squares are 11 and 20 μm measurements from the AFGL Catalog (Price and Walker 1976) for NGC 7023 and NGC 2023, and from the AFGL Supplemental Catalog (Price 1977) for NGC 2068. The open circles are far-infrared measurements from Whitcomb *et al.* (1981) for NGC 7023 and from Harvey, Thronson, and Gatley (1980) for NGC 2023.

of the reflection nebulae observed here, $\sim$1000 K, the high-temperature limit of the heat capacity must be used, $C_V = 3Nk$, where $3N$ is the number of degrees of freedom in the grain. The high-temperature limit is a reasonable approximation as long as the temperature is higher than about one-fifth of the Debye temperature (Kittel 1969), and thus is appropriate even for materials with very high Debye temperatures, such as diamond with a Debye temperature of 2200 K. The value of N will range from the number of molecules in the grain lattice to the number of atoms in the grain lattice, depending on the degree to which the internal vibrational degrees of freedom of molecules in the grain are excited at $\sim$1000 K.

A number of processes may contribute to the excitation of the thermal fluctuations. Absorption of UV photons and chemical reactions between molecules on the grain surface have already been mentioned. Other possibilities are collisions between the grain and atoms, molecules, or other grains; cosmic rays; and runaway chemical reactions among molecules on the grain surface, or "chemical explosions" (Greenberg 1973; d'Hendecourt *et al.* 1982). The efficiency of any excitation process for the thermal fluctuations depends on both the expected rate of the heating events, and the energy of the event available for grain heating. These can be calculated for each possible process, for reasonable assumptions about the physical conditions in the nebulae.

From the observed near-infrared luminosity of the reflection nebulae one can derive a rate R for the heating events of $R = 7 \times 10^{-7} x^{-1} (10^3\ \mathrm{cm}^{-3}/n_\mathrm{H})(1000\ \mathrm{K}/T)\ \mathrm{s}^{-1}$, where x is the mass fraction of grains contributing to the near infrared emission, n_H is the hydrogen density, and T is the grain temperature (Sellgren 1983*b*). Since $x \leq 1$, the minimum rate required for the heating events is 7×10^{-6} to $7 \times 10^{-8}\ \mathrm{s}^{-1}$, for the densities of 10^2–$10^4\ \mathrm{cm}^{-3}$ appropriate to the reflection nebulae. This required minimum rate rules out many possible processes as explanations of the observed near-infrared emission, leaving the processes of photon absorption, gas-grain collisions, and molecular bond formation on grain surfaces.

The most energetic of the processes which occur frequently enough to account for the emission are gas-grain collisions in shock fronts and the absorption of UV photons. Processes occuring in shock fronts can be ruled out, however, on the basis of the spatial distribution, since these hypothetical shocked regions, caused by mass loss from pre–main-sequence stars, would be confined to regions within 15″ of the pre–main-sequence star (Sellgren 1983*b*). In NGC 2023 near infrared emission is seen 3′ north of the central star (Fig. 2),

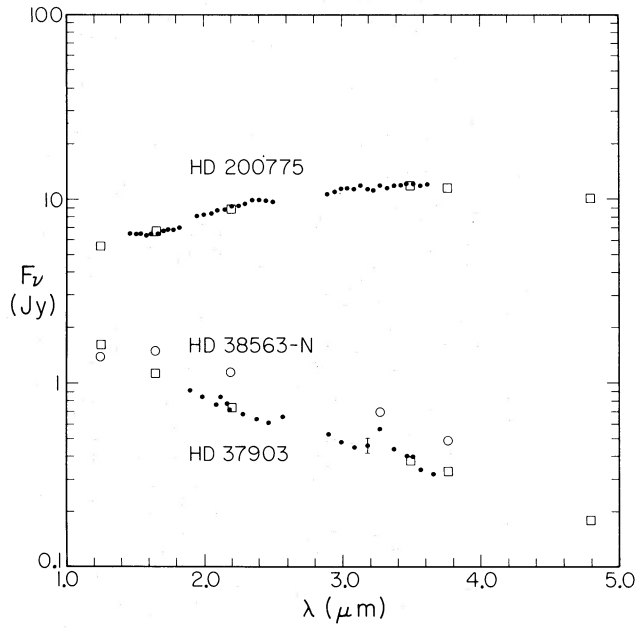

FIG. 9.—The spectra of HD 200775, HD 38563N, and HD 37903, which are, respectively, the illuminating stars of the reflection nebulae NGC 7023, NGC 2068, and NGC 2023. For HD 200775 and HD 37903, filled circles represent spectrophotometry, and open squares broad-band photometry. For HD 38563N open circles represent both broad band photometry, at 1.25, 1.65, 2.2, and 3.8 μm, and a 1% resolution spectrophotometric measurement at 3.3 μm. For HD 200775 the resolution for the spectrophotometry was 5% from 1.5 to 2.5 μm, and 1% from 2.9 to 3.6 μm. The spectrophotometry of HD 37903 is 1% resolution. Error bars representing $\pm 1\ \sigma$ uncertainties are shown only when larger than $\pm 5\%$.

while all the pre–main-sequence stars found at 2.2 μm in this nebula are $\sim 1'$ south of the central star (Paper II). Gas-grain collisions either in molecular cloud material or in small H II regions surrounding the central stars, and bond formation on grain surfaces, provide little energy for grain heating. The model to be described, therefore, assumes UV photons excite the thermal fluctuations.

The high temperatures characteristic of the reflection nebulae, ~ 1000 K, imply very small grain sizes. The number of molecules is determined by comparing the energy of the heating event, taken here to be the photon energy E_{ph}, to the integral of the heat capacity over temperature. Since for T large, $C_V = 3Nk$, a rough estimate of this integral is $E_{ph} = 3Nk\Delta T$, where ΔT is the difference between maximum and minimum temperatures. Thus for $E_{ph} = 10$ eV and $\Delta T = 1000$ K, $N = 30$ molecules. For a lattice spacing of ~ 3 Å this corresponds to a grain radius of ~ 10 Å. A more careful calculation, using the theory outlined by Allen and Robinson (1975), gives $N = 70$ and 90, and radii of 9 and 6 Å, for silicate and graphite grains respectively.

One of the major advantages of this model is that the surface brightness of the near-infrared emission, if excited by UV radiation from the central star, is predicted to follow the distribution of stellar flux throughout the nebula. Since the visual surface brightness of reflected light also depends on the stellar flux at each point, this model naturally predicts the observed agreement between the surface brightness distributions at visual and near-infrared wavelengths. Furthermore, since the peak temperature depends only on the grain size and the energy of the UV photon, the color temperature would be expected to be independent of distance from the central star, as observed.

It is of interest to estimate what the number of small grains required to explain the observations implies about the grain size distribution in the reflection nebulae. One way of investigating this question is to compare the observations with the grain size distribution of Mathis, Rumpl, and Nordsieck (1977, hereafter MRN). This grain size distribution, $n(a)da = n_0 a^{-3.5} da$, where a is the grain radius, extends over the range $a_+ > a > a_-$, where MRN adopted $a_+ = 0.25$ μm and $a_- = 0.005$ μm. Biermann and Harwit (1980) have proposed that the origin of this grain size distribution is grain-grain collisions in the regions, such as red giant atmospheres, where grains form, and find that the $a^{-3.5}$ distribution should extend to grain radii as small as 10 Å. This grain size distribution, extended to smaller grain sizes than considered by MRN, provides good agreement with the observations of reflection nebulae. The expected fraction x of the total dust mass in 10 Å–sized grains, from an extension of the MRN distribution, is $x = 2 \times 10^{-3}$. The fractional dust mass required by the observations, for a rate of photon absorption of 2×10^{-4} s^{-1} and a hydrogen density of 10^3 cm^{-3}, is $x = 3 \times 10^{-3}$ (Sellgren 1983*b*). The fraction of the stellar luminosity absorbed by grains of radius ~ 10 Å and reradiated in the near infrared, compared to the total stellar luminosity absorbed by dust and reradiated at all infrared wavelengths, is observed to be $\sim 10^{-2}$. The value expected for a MRN distribution, extended to smaller grain sizes, is $\sim 4 \times 10^{-3}$. The good agreement of the number of grains required to explain the near-infrared emission with the number expected from a MRN size distribution is encouraging and demonstrates that quite reasonable numbers of small grains are required to account for the observations.

An obvious concern when grain sizes this small are involved is whether heat capacities and optical constants measured for bulk materials will apply to grains of this size. Martin (1973) finds that calculations of the heat capacity and absorption coefficients of ionic crystals containing 64 atoms differ very little from calculations for infinite crystals. Similarly, Kreibig (1974) finds that bulk optical constants for metals need only minor modifications to provide agreement with measurements of metal particles containing as few as 50 atoms. The differences between the small particle and bulk heat capacities are much smaller than the uncertainties in the calculations of this paper due to the use of the Debye approximation or due to the unknown composition of the grains. The differences in the optical constants also are not important for the calculations of this paper but may eventually imply interesting effects in the spectra of these grains, such as the increasing importance of surface phonon modes at far-infrared wavelengths.

c) Implications

The model described in § IV*b*, while not unique, does explain many of the observed features of the near-infrared emission of these three visual reflection nebulae. The grain sizes required to explain peak temperatures ~ 1000 K are uncomfortably small, $a \sim 10$ Å, but the numbers of these grains required are consistent with the extrapolation of the MRN grain size distribution to smaller grain sizes.

It seems likely that the observed near-infrared emission exists in other regions but has not been detected previously due to the small fraction, $\sim 10^{-2}$, of the total luminosity involved. This small contribution is easily masked by other near-infrared emission mechanisms. If the emission is excited by UV photons, then it should be found only near O and B stars, the hotter of which have substantial H II regions which have associated free-free emission as well as equilibrium thermal emission from dust heated by trapped Ly-α radiation. Most cooler stars probably produce too few UV photons to produce observable amounts of the near-infrared emission. The reflection nebulae observed were originally selected for having the most luminous central stars possible without having significant H II regions, as well as having modest amounts of dust. Thus these sources represent a special set of physical conditions where the amount of UV radiation is sufficient to produce observable near-infrared emission from the thermally fluctuating small grains, yet insufficient to ionize an H II region which masks the near-infrared emission.

One feature of the proposed grains of radius ~ 10 Å is that they are difficult to detect except through their thermal fluctuations. They represent only a small fraction of the total dust mass. Similarly, they contribute little to the extinction at visual and ultraviolet wavelengths. This is because grains absorb efficiently only at wavelengths comparable to and shorter than $2\pi a$, i.e., for $a = 10$ Å, the wavelength of soft X-rays, a wavelength region where processes other than grain extinction dominate the absorption.

The constancy of the 3.3 μm feature-to-continuum ratio in the three visual reflection nebulae (Paper I) suggests that the feature is associated with the continuum. One possible explanation is that the 3.3 μm feature is due to fluorescence

(Allamandola, Greenberg, and Norman 1979), so that both the feature emission and the continuum emission from the thermally fluctuating grains is proportional to the incident UV stellar flux. The similarity of α_{UV}, the required conversion efficiency of UV photons to 3.3 μm feature photons, in the reflection nebulae to the values of α_{UV} found in other sources (Dwek *et al.* 1980) where the fluorescence model fails, however, argues against this explanation. Another possibility is that the 3.3 μm feature, as well as the continuum, is due to thermal emission from thermally fluctuating grains. Sellgren (1981) has argued that the 3.3 μm emission in the Orion nebula arises in the H II region–molecular cloud interface, and that the 3.3 μm emitting material is destroyed when heated to high temperatures in the vicinity of the Trapezium. This suggests the 3.3 μm emitting grains in the reflection nebulae may be somewhat larger grains ($\sim$15 Å) than those producing the 3 μm continuum, with correspondingly lower peak temperatures ($\sim$300 K). In sources where the equilibrium grain temperatures are high enough to produce the observed 3.3 μm emission, such as Orion, the 3.3 μm feature would arise mainly from grains with $a \sim 50$ Å, as proposed by Dwek *et al.* (1980), since the smaller grains ($a \sim$ 10–15 Å) absorb a smaller fraction of the heating radiation.

While the 3.3 μm emitting material may be volatile, the grains producing the near-infrared continuum emission by thermal fluctuations must be relatively refractory. The time scale for two UV photons being absorbed by a small grain, close enough in time to raise the peak temperature to twice the peak temperature caused by a single UV photon, is $\sim 10^2$ yr. Thus the thermal fluctuation model requires that the continuum emitting grains survive occasional heating to $\sim$2000 K. The rate of absorption of three UV photons simultaneously is negligibly small.

V. SUMMARY

The observations presented in this paper and in Paper I show the following results:

1. Near-infrared emission is found in three visual reflection nebulae, extended over 0.4–0.9 pc. The emission in NGC 7023 and 2023 peaks near the visual illuminating star and falls off with projected distance from the central star. The emission in NGC 2068 has no strong peak and has approximately constant surface brightness across the nebula.

2. The energy distribution of each nebula shows no evidence for any dependence on position in the nebula or offset from the central star. The spectra of the three nebulae are very similar.

3. The spectrum with 1%–5% resolution of the nebulae consists of a smooth continuum from 1.5 to 3.7 μm, except for emission features at 3.3 and 3.4 μm. The continuum from 1.25 to 4.8 μm can be characterized by a color temperature of $\sim$1000 K. The feature-to-continuum ratio of the 3.3 μm emission feature is 6.

4. The spatial distribution of near infrared surface brightness in NGC 7023 and NGC 2023 agrees extremely well with that of visual reflected light.

The following model may be able to account for the observations:

1. Thermal emission from very small grains undergoing thermal fluctuations could explain the high observed color temperatures. These small grains have low heat capacities, so that they momentarily reach high temperatures after being excited by absorption of UV photons, chemical reactions on their surface, or collisions.

2. The most efficient excitation mechanism, in terms of frequency of occurence and available heating energy, is absorption of UV photons.

3. The required number of molecules in the grain, to reach a color temperature of 1000 K after absorption of a 10 eV photon, is $\sim$70–90 molecules. This corresponds to a grain radius of $\sim$10 Å.

4. This mechanism naturally explains the good agreement of near-infrared and visual surface brightness distributions, since both the rate of excitation of the thermal fluctuations and the visual reflected light depend directly on the incident stellar flux. Furthermore, the peak grain temperature attained is predicted to be independent of distance from the star, in agreement with the observed constancy of the color temperature throughout these nebulae.

5. The mass of grains required is a small fraction, $\sim 10^{-3}$, of the total mass of grains, and is consistent with an extrapolation of the grain size distribution of Mathis, Rumpl, and Nordsieck (1977) to smaller grain sizes. The ratio of the near-infrared to total infrared luminosities observed is also consistent with the ratio of UV absorption cross sections predicted for this grain size distribution.

I thank the staff of Mount Wilson Observatory for their hospitality during my interminable observing runs; my night assistants at Mount Wilson Observatory, J. Frazer and H. Lanning; and my telescope operators at the Infrared Telescope Facility, C. Kaminski and D. Griep. Additional assistance with observations was provided by G. Berriman, R. Capps, H. L. Dinerstein, J. H. Lacy, M. Malkan, Y. Pendleton, A. Rosenthal, B. T. Soifer, M. W. Werner, S. E. Whitcomb, and R. L. White. I especially thank S. E. Whitcomb, who collaborated on the 2.2 μm observations of NGC 7023. I thank the Infrared Telescope Facility for providing their RC-2 InSb system; E. Erickson for the loan of a 2–4 μm circular variable filter wheel; G. Neugebauer for the use of, and K. Matthews for the construction and maintenance of, Caltech infrared group equipment; an anonymous referee for useful suggestions; and A. N. Witt and A. Sargent for communicating results prior to publication. Useful conversations were held with S. E. Whitcomb, R. L. White, M. Jura, M. W. Werner, A. N. Witt, L. Allamandola, F. Baas, H. L. Dinerstein, B. T. Soifer, and G. Neugebauer. This research was supported by NASA and NSF.

REFERENCES

Aitken, D. K. 1981, in *IAU Symposium 96, Infrared Astronomy*, ed. C. G. Wynn-Williams and D. P. Cruikshank (Dordrecht: Reidel), p. 207.
Allamandola, L. J., Greenberg, J. M., and Norman, C. A. 1979, *Astr. Ap.*, **77**, 66.
Allen, M., and Robinson, G. W. 1975, *Ap. J.*, **195**, 81.
Beckwith, S., Evans, N. J., Becklin, E. E., and Neugebauer, G. 1976, *Ap. J.*, **208**, 390.
Biermann, P., and Harwit, M. 1980, *Ap. J.*, **241**, 405.
d'Hendecourt, L. B., Allamandola, L. J., Baas, F., and Greenberg, J. M. 1982, *Astr. Ap.*, **109**, L12.

Duley, W. W. 1973, *Nature Phys. Sci.*, **244**, 57.
Dwek, E., Sellgren, K., Soifer, B. T., and Werner, M. W. 1980, *Ap. J.*, **238**, 140.
Elias, J. H. 1978, *Ap. J.*, **223**, 859.
Elias, J. H., Frogel, J. A., Matthews, K., and Neugebauer, G. 1982, *A.J.*, **87**, 1029.
Greenberg, J. M. 1973, in *Molecules in the Galactic Environment*, ed. M. A. Gordon and L. E. Snyder (New York: John Wiley).
Greenberg, J. M., and Hong, S. S. 1974, in *IAU Symposium 60, Galactic and Radio Astronomy*, ed. F. Kerr and S. C. Simonson (Dordrecht: Reidel), p. 155.
Guetter, H. H. 1979, *A.J.*, **84**, 1846.
Harvey, P. M., Thronson, H. A., and Gatley, I. 1980, *Ap. J.*, **235**, 894.
Harwit, M. 1975, *Ap. J.*, **199**, 398.
Kittel, C. 1969, *Thermal Physics* (New York: John Wiley).
Kreibig, U. 1974, *J. Phys. F*, **4**, 999.
Lee, T. A. 1968, *Ap. J.*, **152**, 913.
Martin, T. P. 1973, *Phys. Rev. B*, **7**, 3906.
Mathis, J. S., Rumpl, W., and Nordsieck, K. H. 1977, *Ap. J.*, **217**, 425 (MRN).
Neugebauer, G. 1982, private communication.
Neugebauer, G., Oke, J. B., Becklin, E. E., and Matthews, K. 1979, *Ap. J.*, **230**, 79.
Neugebauer, G., Soifer, B. T., Matthews, K., Margon, B., and Chanan, G. A. 1982, *A.J.*, **87**, 1639.
Price, S. D. 1977, AFGL-TR-77-0160.
Price, S. D., and Walker, R. G. 1976, AFGL-TR-76-0208.
Purcell, E. M. 1976, *Ap. J.*, **206**, 685.
Sellgren, K. 1981, *Ap. J.*, **245**, 138.
———. 1983*a*, *A.J.*, **88**, 985 (Paper II).
———. 1983*b*, Ph.D. thesis, California Institute of Technology.
Sellgren, K., Werner, M. W., and Dinerstein, H. L. 1983*a*, *Ap. J.* (*Letters*), **271**, L13 (Paper I).
———. 1983*b*, in preparation.
Strom, K. M., Strom, S. E., and Vrba, F. J. 1976, *A.J.*, **81**, 308.
Viotti, R. 1969, *Mem. Soc. Astr. Ital.*, **40**, 75.
Whitcomb, S. E., Gatley, I., Hildebrand, R. H., Keene, J., Sellgren, K., and Werner, M. W. 1981, *Ap. J.*, **246**, 416.
Willner, S. P. 1983, in *Galactic and Extragalactic Infrared Spectroscopy, ESLAB Symposium No. 16*, ed. M. F. Kessler (Dordrecht: Reidel), in press.
Witt, A. N., and Cottrell, M. J. 1980, *A.J.*, **85**, 22.
Witt, A. N., Schild, R. E., and Kraiman, J. B. 1983, in preparation.
Zellner, B. 1970, Ph.D. thesis, University of Arizona.

K. SELLGREN: Space Telescope Science Institute, Homewood Campus, Baltimore, MD 21218